

Nonresonant tunneling carrier transfer in bilayer asymmetric InAs/GaAs quantum dotsYu. I. Mazur,* Zh. M. Wang, G. G. Tarasov,[†] and G. J. Salamo
*Department of Physics, University of Arkansas, Fayetteville, Arkansas 72701, USA*J. W. Tomm and V. Talalaev
*Max-Born-Institut für Nichtlineare Optik und Kurzzeitspektroskopie, Max-Born-Strasse 2A, 12489 Berlin, Germany*H. Kissel
Ferdinand-Braun-Institut für Höchstfrequenztechnik, Gustav-Kirchhoff-Strasse 4, 12489 Berlin, Germany
(Received 15 October 2004; revised manuscript received 1 March 2005; published 13 June 2005)

Carrier transfer in InAs/GaAs asymmetric quantum dot pairs has been studied by means of continuous-wave and time-resolved photoluminescence in a bilayer InAs/GaAs quantum dots system. The dependence of the tunneling time on the thickness of the separation layer is determined and the tunneling time is found to span the range from 250 to 2500 ps. A microscopic model of carrier transfer, including nonresonant electron tunneling from a direct into a cross exciton state, with subsequent generation of two direct excitons in adjacent quantum dot layers, is proposed.

DOI: 10.1103/PhysRevB.71.235313

PACS number(s): 78.55.Cr, 78.47.+p, 78.66.Fd

I. INTRODUCTION

Many proposed electronic or optoelectronic applications of quantum dots (QDs) require uniformity in performance and consequently in both QD size and shape.¹ One promising approach pursued to achieve the required homogeneity is the growth of multiple layers of QDs.² In this approach, layers of three-dimensional (3D) islands are each separated by a layer of a material that acts as both a barrier and a spacer layer. Control over the spacer layer thickness has been shown to influence the degree of strain transmitted from the first QD layer into the subsequent separation layer, so that nucleation of the second QD layer is vertically ordered above the first. In fact, a significant degree of both vertical and lateral ordering has been achieved when multilayers of QDs are prepared in this way.^{2,3}

Given some early success with this approach it has become interesting to investigate the behavior of organized arrays of QDs. Developing an understanding of such structures is not necessarily easy, however, since each dot layer must be close enough to influence another one, making tunneling between dots more complicated. In order to explore the behavior of 3D arrays, some recent investigations have focused on the simpler structure consisting of only two QD layers separated by one spacer layer.⁴⁻¹¹ For example, a recent paper¹² has reported on an investigation of bilayers of InAs QDs with GaAs as the barrier, giving photoluminescence (PL) up to $\approx 1.4 \mu\text{m}$ at room temperature for a second layer with a reasonable density of $2 \times 10^{10} \text{ cm}^{-2}$ and a remarkably narrow PL linewidth of as low as 14 meV.

For a bilayer QD structure, the two layers can either be grown identically or under different conditions. Using different InAs deposition values, growth temperature, or annealing time for each QD layer, a vertically stacked pair of unequal sized QDs can be realized. Such a system has been called an “asymmetric QD pair” (AQDP) in analogy to the extensive work on asymmetric double quantum-well (ADQW) systems.⁴ Not only can studies on the AQDP lead to a better

understanding of multilayered QD structures and hence more control over uniformity of size and shape, but they may also prove to be useful for applications. For example, AQDPs sharing a single electron in each pair have attracted great interest in connection with the realization of quantum bits and quantum computation.¹

Of course a good understanding of the bilayer AQDP requires exploration of many phenomena. One important characteristic of such a system is the tunneling time of carriers between pair dots, which can be investigated by either continuous-wave (cw) or transient PL. While both approaches can give valuable insight, transient studies provide clues on the inner dynamics and give accurate values for the tunneling times of electrons and holes. In this paper, we report on detailed cw PL as well as time-resolved PL studies on carrier tunneling transfer among vertically aligned double-stacked InAs/GaAs QD layers.

II. SAMPLE CHARACTERIZATION

The AQDP samples explored here were grown using a solid-source molecular beam epitaxy chamber coupled to an ultrahigh vacuum scanning tunneling microscope (STM). The structures consist of two InAs layers. Each sample was grown on a GaAs (001) substrate, with a $0.5 \mu\text{m}$ GaAs buffer layer and 10 min annealing at 580°C to provide a nearly defect-free atomically flat surface. The seed QD layer is then grown by depositing 1.8 monolayers (ML) of InAs under an As_4 partial pressure of 8×10^{-6} Torr at a substrate temperature of 500°C . This is followed with either 30, 40, 50, or 60 ML of GaAs spacer (d_{sp}) deposited on top of the seed QD layer. The second QD layer is then added through deposition of 2.4 ML InAs. Each sample for optical studies was finally capped with a 150 ML GaAs layer. The growth rates of InAs and GaAs for all layers were 0.1 and 1.0 ML/s, respectively.

The samples were structurally characterized by plan-view STM and cross-sectional transmission electron microscopy

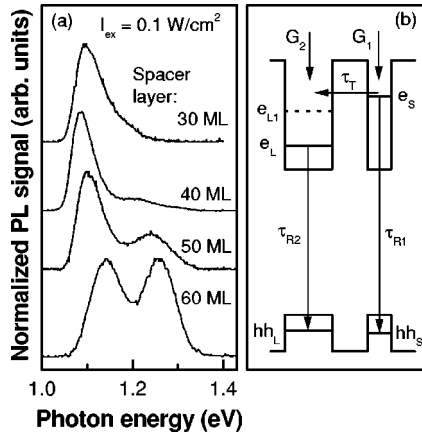


FIG. 1. (a) Low excitation density cw PL spectra at $T=10$ K for 1.8/2.4 ML AQDP samples with various spacer thickness. (b) Schematic representation of processes contributing to carrier populations in SQD and LQD ensembles. Photoexcitation of carriers is represented by $G1$ and $G2$, tunneling time for electrons is τ_T , and recombination lifetimes are τ_{R1} and τ_{R2} for SQDs and LQDs, respectively.

(XTEM). The STM statistical analysis indicates a size distribution for the QDs with (4.0 ± 1.5) nm for the height, (20 ± 3) nm for the width, and a dot density of about $4.5 \times 10^{10} \text{ cm}^{-2}$ in the seed layer. The dot density in the second layer is variable over the range from 2.5×10^{10} to $4.0 \times 10^{10} \text{ cm}^{-2}$ with increasing d_{sp} . Meanwhile, the second layer 3D islands are nearly twice in volume of the seed islands (for $d_{sp}=30$ ML) due to additional deposition, as well as the influence of the strain field from the seed layer.^{4,10} The resulting growth was a vertically correlated bilayer QD structure with different sized dots in each layer. However, the correlation is not complete, and a part (α) of the QDs of the seed layer, as well as the part of the QDs of the second layer is still uncoupled. XTEM statistical analysis was used to determine the dependence of the AQDP fraction [the correlation degree $(1-\alpha)$] of the total QDs density of the seed layer on the d_{sp} value to be $1-\alpha=0.95, 0.70, 0.50,$ and 0.10 for $d_{sp}=30, 40, 50,$ and 60 ML, respectively.

III. CW PHOTOLUMINESCENCE

The cw PL was studied by using the 514.5-nm line of an Ar^+ laser for GaAs excitation, spanning excitation densities from 0.01 to 40 W/cm^2 . The samples were mounted in a close-cycle cryostat, which allowed measurements in the temperature range from 10 to 300 K. The PL signal was detected with a liquid-nitrogen-cooled Ge photodiode using phase-sensitive detection techniques.

Figure 1 shows the cw PL spectra for AQDPs, with InAs coverage of 1.8 and 2.4 MLs for the seed and second layers, respectively, as a function of spacer thickness at a low excitation density (I_{ex}) of about 0.1 mW/cm^2 . As expected^{3,4} the PL spectrum for $d_{sp}=30$ ML shows a single, slightly asymmetric Gaussian shaped peak (P_{sec}) at 1.09 eV, which is the emission energy expected from the large QDs (LQDs) in the

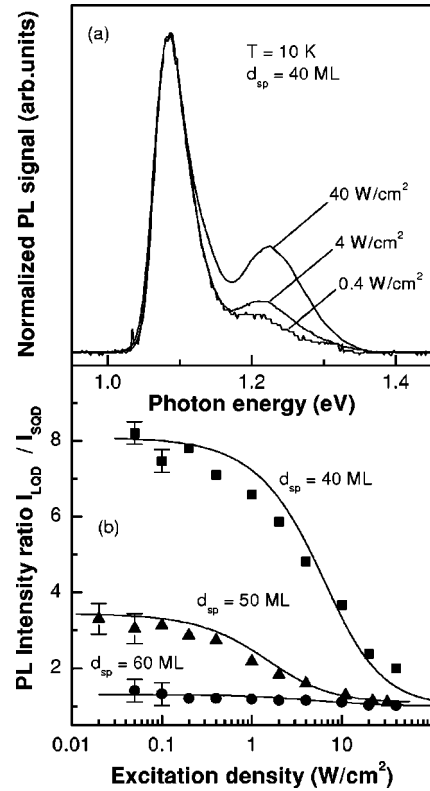


FIG. 2. (a) The normalized PL spectra of a sample with $d_{sp}=40$ ML for different I_{ex} . (b) PL peak intensity ratio I_{LQD}/I_{SQD} of the LQD and SQD PL spectra vs excitation level for various barrier thicknesses. The fit with Eqs. (2) is shown by solid lines.

second layer. In this case the tunneling time (τ_T) from the seed layer dots to the second layer is apparently so fast compared to the radiative lifetime of the small QDs (SQDs) (τ_{R1}) (τ_T is less than τ_{R1}) that very little PL from the seed layer is observed. With increasing d_{sp} , however, an additional PL peak becomes evident on the high-energy side at 1.27 eV, resulting in a clear double peak structure for the 50 and 60 ML spacer samples. This high-energy peak (P_{seed}) coincides with the QD PL peak observed for single-layer samples with a 1.8 ML InAs deposition¹⁰ and is therefore attributed to the emission from SQDs. The apparent increase in the PL yield of the SQDs with increasing spacer thickness is also expected due to the decreasing electronic coupling and, consequently, decreasing carrier transfer probability between AQDPs.

Perhaps less expected is the fact that the cw PL spectra as a function of d_{sp} reveal a significantly different PL behavior between the SQD and LQD peaks as a function of the excitation density I_{ex} . Investigation of PL spectra in our samples over a wide range of excitation densities covering four orders of magnitude as well as thorough line-shape analysis convince us that we are still below the intensity needed to excite higher energy levels. Therefore contributions from excited states of the LQDs are ignored in our cw PL experiments. Figure 2(a) plots normalized PL spectra, as a function of I_{ex} , for the sample with $d_{sp}=40$ ML. The peak intensity ratio I_{LQD}/I_{SQD} , as a function of I_{ex} [Fig. 2(b)], shows a weak dependence on I_{ex} for $d_{sp}=60$ ML, when the seed and sec-

ond QD layers are nearly decoupled, but a significant influence for a d_{sp} of 40 ML when the coupling is strong. For the strong coupling case, at high I_{ex} , the filling of the energy levels in the LQDs understandably reduces the carrier transfer from the ground state of the SQDs thus increasing the population of this state and decreasing the ratio I_{LQD}/I_{SQD} as shown in Fig. 2(b). Here again, a similar observation has been reported for nonresonant electron and hole tunneling in coupled InGaAs/InP quantum wells.^{13,14} In that case, a space-charge buildup, due to asymmetric electron and hole tunneling, is assumed to lead to bending and shifting of the energy levels of the wells resulting in changes in the distribution of the population in the energy levels¹³ and hence the PL ratio. However, in the case of the AQDPs studied here, a similar space charge buildup explanation is not reasonable due to the limited number of QDs and a large energetic distance between the ground states of electron-hole transitions (about 120 meV) of the seed and second QD layers. There is also no PL evidence for an energy level shift. Rather, for AQDPs we attribute the decrease in carrier transfer probability with elevating I_{ex} to a decrease of available free ground states in the larger QDs in the second layer. This is also consistent with the greater probability of level filling for QDs.

Figure 1(b) presents a schematic energy level diagram for the AQDP structures. We assume a simple three-level model for this structure in order to uncover the behavior of the tunneling time τ_T and radiative lifetimes of the SQDs and LQDs, τ_{R1} and τ_{R2} , respectively. Within this model the observed decrease in carrier transfer probability can be understood as state filling due to increasing I_{ex} . In addition, for the samples with $d_{sp} \leq 50$ ML, when τ_T becomes smaller than τ_{R1} and $\tau_{R1} \leq \tau_{R2}$,^{15,16} carrier tunneling from a SQD to the LQD, in steady state, is limited by τ_{R2} . This scenario can be treated within a three-level model [see Fig. 1(b)] approximation, using the following rate equations:

$$\begin{aligned} \frac{dn_1(t)}{dt} &= -\frac{n_1(t)}{\tau_{R1}} - \frac{n_1(t)[N_2 - n_2(t)]}{N_2\tau_T} + G_1[N_1 - n_1(t)]/N_1, \\ \frac{dn_2(t)}{dt} &= -\frac{n_2(t)}{\tau_{R2}} + \frac{n_1(t)[N_2 - n_2(t)]}{N_2\tau_T} + G_2[N_2 - n_2(t)]/N_2. \end{aligned} \quad (1)$$

Here $n_1(t)$ and $n_2(t)$ represent the carrier densities at time t in the lowest energy levels of the SQDs and the LQDs, respectively. N_2 is the total number density of LQDs that are coupled to an equal number of SQDs N_1 in the AQDPs. The factor $n_1(t)[N_2 - n_2(t)]/N_2$ defines the fraction of SQDs for which tunneling within AQDP takes place since the corresponding LQDs are empty. G_1 and G_2 are the carrier generation rates for the SQDs and the LQDs, respectively. The set of equations (1) takes into account the saturation of the carrier trap into the SQDs and LQDs states, respectively.

Applying Eqs. (1) for the steady state case, $dn_1/dt=0$, $dn_2/dt=0$, we get the solutions

$$n_1^S = N_1 - \tau_{R1}(-B - \sqrt{B^2 - 4AC})/2A,$$

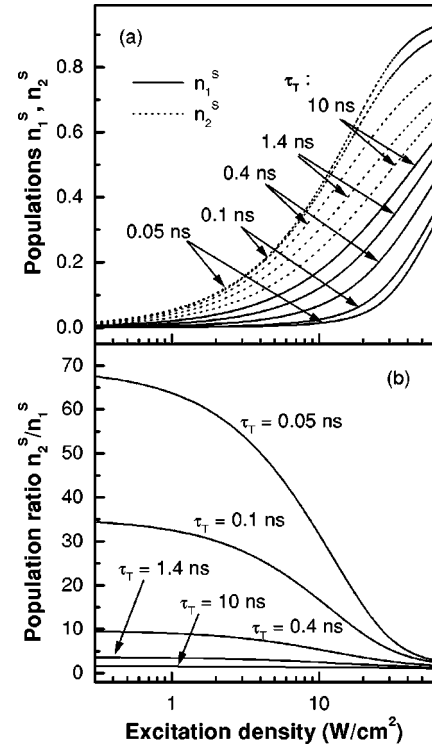


FIG. 3. The n_1^S and n_2^S dependences vs excitation density (a), and the ratio n_2^S/n_1^S (b) calculated from Eqs. (2) for different tunneling time τ_T and fixed relaxation times for SQDs $\tau_{R1}=1.4$ ns and LQDs $\tau_{R2}=1.7$ ns, respectively. The generation rates G_1 and G_2 are taken equal.

$$n_2^S = N_2 - \tau_{R2}[\gamma - \delta(N_1 - n_1^S)/\tau_{R1}], \quad (2)$$

with $A = (\tau_{R1}\tau_{R2}/N_2\tau_T)\delta$, $B = -1 - G_1\tau_{R1}/N_1 - (\gamma + \delta N_1/\tau_{R1})A/\delta$, and $C = \gamma(N_1\tau_{R2}/N_2\tau_T) + N_1/\tau_{R1}$, where $\gamma = (N_1/\tau_{R1} + N_2/\tau_{R2})/(1 + G_2\tau_{R2}/N_2)$ and $\delta = (1 + G_1\tau_{R1}/N_1)/(1 + G_2\tau_{R2}/N_2)$.

Equation (2) describes saturation in the AQDPs system resulting from the limitation of carrier transfer out of the SQDs into the LQDs as the population of the LQDs ground state becomes large. This effect becomes pronounced under a substantial elevation of the excitation density. For example, Fig. 3 gives the n_1^S and n_2^S dependence on the excitation density for various rates of carrier transfer ($1/\tau_T$) within the AQDP. The figure shows that the ratio n_2^S/n_1^S (related to the ratio I_{LQD}/I_{SQD} for PL intensities) is also a function of the excitation density.

For our excitation wavelength, we assume equal excitation rates for both the SQDs and LQDs.⁴ In the range of low excitation densities [Fig. 3(a)], it can be seen that the states of the LQDs populate substantially faster than states of the SQDs in the AQDPs due to the additional flow of carriers from the SQDs. When tunneling takes place the ratio n_2^S/n_1^S tends to the limiting value of $\tau_{R2}(\tau_T + 2\tau_{R1})/(\tau_{R1}\tau_T)$ as $G_1, G_2 \rightarrow 0$ in the limit of extremely low excitation densities [Fig. 3(b)]. If the tunneling carrier transfer is negligible ($\tau_T \rightarrow \infty$) this ratio tends to the value τ_{R2}/τ_{R1} , while in the case of rapid carrier escape from the SQDs states ($\tau_T \rightarrow 0$)

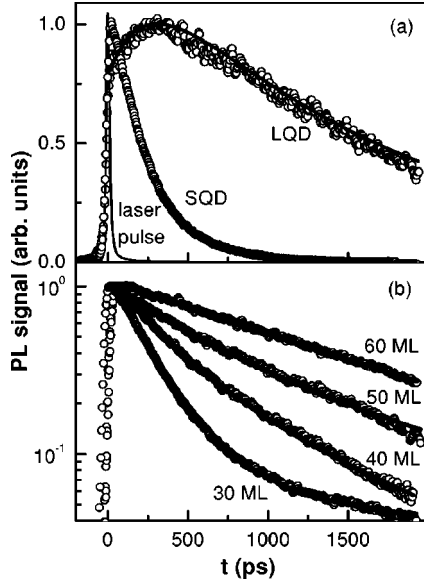


FIG. 4. (a) Normalized PL transients for SQDs and LQDs for an AQDP sample with a spacer thickness of 30 ML. The detection energies are 1.25 and 1.094 eV for SQDs and LQDs, respectively. (b) Normalized PL transients for SQD for AQDP samples with various spacer thicknesses. The detection energy is at 1.25 eV. The calculated dependences shown with solid lines where found from the least-squares fit by Eqs. (4) and (5) with the correlation parameters $(1-\alpha)$ taken to be 0.95, 0.75, 0.55, and 0.10 for the $d_{sp}=30, 40, 50,$ and 60 ML, respectively.

the ratio n_2^S/n_1^S tends to the limit $2\tau_{R2}/\tau_T$, which can be very large. On the other hand, if the excitation densities are high enough ($G_1, G_2 \rightarrow \infty$), the populations n_1^S and n_2^S are saturated for both the SQDs and the LQDs.

IV. TRANSIENT PHOTOLUMINESCENCE

Indeed, although the cw PL spectra as a function of d_{sp} provides significant insight into tunneling from the SQD layer to the LQD layer, they do not allow a direct determination of the tunneling time, which may be one of the reasons for the large spread in reported values. For the determination of these important physical parameters, transient PL measurements are of crucial importance. Figure 4(a) gives the time decay curves of SQDs and LQDs for $d_{sp}=30$ ML while Fig. 4(b) gives transient PL signals of the fundamental exciton transition in the SQDs for different d_{sp} . Optical excitation for the transient PL measurements was provided by 80-fs pulses at $\lambda=732$ nm from a mode-locked Ti:sapphire laser producing an optical pulse train at 82 MHz and an excitation density that was varied between 10^9 and 2×10^{13} photons/(pulse \times cm 2). To avoid excited state emission complications to the PL transient spectra we insured that our excitation density was always well below saturation levels by restricting the PL emission to a range that was linear with the excitation density. Experimentally this range was between 10^9 and 5×10^{11} photons/(pulse \times cm 2) and is consistent with previous studies.¹⁶ Therefore for the experiments discussed here we avoided excited state

emission by limiting the excitation density from 10^9 to 10^{11} photons/(pulse \times cm 2). Transient PL measurements were taken using a monochromator and a synchroscan streak camera equipped with an infrared enhanced S1 cathode with an overall time resolution of 15 ps. For all samples investigated here, the PL transients were measured at the position of the PL maximum for both the SQDs and the LQDs. In addition, we chose a low I_{ex} at 5×10^9 photons/(pulse \times cm 2) as a compromise between what is needed to provide sufficiently high signal-to-noise ratios and the low-excitation levels required to avoid excited-state PL contributions. As shown in Fig. 4(b), the transients for SQDs of different samples cannot uniformly be fitted by one-decay time that decreases with increasing d_{sp} . In addition, the transient data for the LQDs indicate a very different behavior in comparison with the SQD transient PL. The observed delayed rise in the PL transients of the QDs are also observed for single dot layers.^{17,18} These delays are the result of relaxation from the excited states to the ground state combined with Pauli blocking¹⁷ or intralayer carrier transfer between the ground states of QDs in a dense QD array.¹⁸ However, in our case of low excitation densities and low QDs density these mechanisms are unlikely and we relate the delayed rise of LQD PL to interdot carrier transfer due to tunneling from seed and second layers. This is evidenced by the fact that the LQDs PL increases with approximately the same time constant as the decrease of the SQD PL. Moreover, with increasing d_{sp} , and correspondingly increasing τ_T , this delayed maximum becomes much less pronounced and practically vanishes for $d_{sp}=60$ ML. These experimental observations are in full agreement with the predictions of Eqs. (1), which can be modified for the case of a δ -like excitation and extremely low population of the QDs ground states ($n_1 \ll N_1, n_2 \ll N_2$). In order to apply Eqs. (1) we assume that intralayer carrier capture into localized QD states is significantly faster (~ 5 ps) than the excitation rate.⁴ The intralayer and intradot carrier relaxation (transferring the captured carriers in the ground QD states) is also assumed faster than the excitation transfer processes and radiative recombination.⁴ In this case the radiative recombination and the excitation transfer between localized QD states determine the observed PL behavior. Tunneling originates in the ground state of SQDs with the tunneling time τ_T . For a very thin spacer layer (<30 ML) the estimated interdot transfer time is comparable with the time of intradot relaxation. In this case, the calculated τ_T value estimated gives only an upper limit. However, under these approximations the rate equations (1) transform into

$$\begin{aligned} \frac{dn_1(t)}{dt} &= -\frac{n_1(t)}{\tau_{R1}} - \frac{n_1(t)}{\tau_T}, \\ \frac{dn_2(t)}{dt} &= -\frac{n_2(t)}{\tau_{R2}} + \frac{n_1(t)}{\tau_T}. \end{aligned} \quad (3)$$

These equations can be immediately integrated under the initial conditions of $n_1(t=0)=n_1(0)$ and $n_2(t=0)=n_2(0)$, as provided by a δ -like excitation at $t=0$, to yield the expressions of interest:

$$n_1(t) = n_1(0)e^{-t/(\tau_{R1} + \tau_T)}$$

and

$$n_2(t) = [n_2(0) + Dn_1(0)]e^{-t/\tau_{R2}} - Dn_1(0)e^{-t/(\tau_{R1} + \tau_T)}, \quad (4)$$

where $D = \tau_{R1}\tau_{R2}/[\tau_{R1}\tau_{R2} + \tau_T(\tau_{R2} - \tau_{R1})]$. The PL decay time for the SQDs τ_{PL} is therefore given by $\tau_{PL} = \tau_{R1}\tau_T/(\tau_{R1} + \tau_T)$. Meanwhile, the recombination lifetime τ_{R1} of the SQDs can be found experimentally since it can be taken equal to that measured τ_{R1}^{ref} from the reference single QD layer sample of appropriate QDs density.

V. DISCUSSION

Up to now to describe the AQDPs kinetics and cw experiments we have considered a fully correlated system where all of the SQDs of seed layer form the AQDPs with the LQDs of second layer. In practice there exist a certain fraction, α , of the SQDs that are not coupled to any LQD in the second layer. Likewise, there will be a certain fraction β of LQDs that are not coupled to any SQD in the seed layer. Intuitively it is clear that $\alpha \geq \beta$ in bilayer structures and the magnitude of α and β must depend on the d_{sp} thickness. Indeed, XTEM statistical analysis gives the correlation factor $(1 - \alpha)$ of ~ 0.95 , ~ 0.70 , ~ 0.50 , and ~ 0.10 for $d_{sp} = 30, 40, 50$, and 60 ML, respectively. The carriers in noncorrelated QDs in each layer are assumed to relax independently of the AQDPs and each other (no lateral coupling) due to the low QDs densities in the samples under investigation. Therefore in what follows we add the PL contribution of the noncorrelated QDs additively to the PL yield from AQDPs. Then one finds for the SQDs:

$$n_1^{total}(t) = n_1^{total}(0)\{\alpha e^{-t/\tau_{R1}} + (1 - \alpha)e^{-t/(\tau_{R1} + \tau_T)}\}, \quad (5)$$

where n_1^{total} and n_2^{total} are the densities of optically excited QDs from the total dot densities n_1^{total} and n_2^{total} measured by STM in the seed and second layers, respectively.

Measuring the transient PL for the seed layer at the maximum of the emission band of SQDs and taking into account the independently determined $\tau_{R1} = \tau_{R1}^{ref}$ and $(1 - \alpha)$ values we can calculate the τ_T value for all of the samples under investigation and uncover the relation $\tau_T = f(d_{sp})$. It is worth noting that the procedure developed here for determining τ_T from the transient PL data gives τ_T values that are substantially different from those cited in bilayer experiments that do not account for the contribution from noncorrelated QDs.^{4,12,19}

Using the determined values of τ_T , τ_{R1} , and taking τ_{R2} as a fitting parameter for the experimentally measured transients for LQDs [see Fig. 4(a)], the relaxation time τ_{R2} is calculated. The result is particularly interesting for the $d_{sp} = 30$ ML sample where the contribution of the noncorrelated LQDs is negligibly small.

Possessing τ_T , τ_{R1} , and τ_{R2} for all samples we can now calculate the dependence of I_{LQD}/I_{SQD} on the excitation density and compare with the result from the cw measurements. Equations (2) show good agreement with the experimental data [Fig. 2(b)], especially if one considers that the experimental accuracy in determining the SQDs PL is limited at

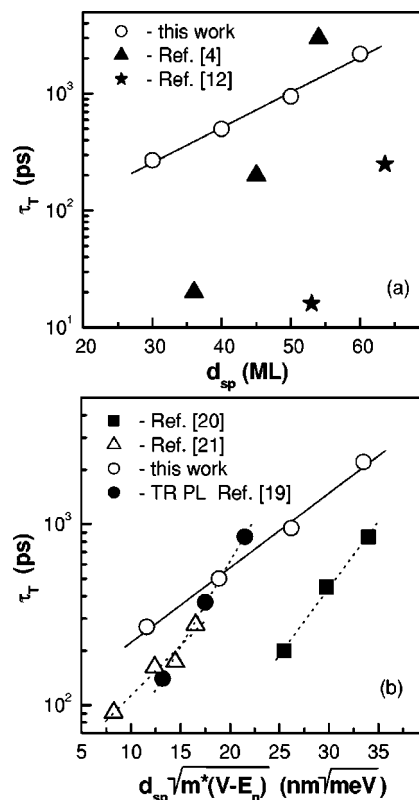


FIG. 5. (a) Tunneling time (open circles) deduced from the SQD's PL transient as a function of barrier width. The solid line is fitted to tunneling times by the least-square method. The data of tunneling times for the similar AQDP systems (closed triangles: Ref. 4; stars: Ref. 12) estimated from cw PL measurements are shown. (b) Comparison of nonresonant electron tunneling times as a function of the effective barrier width observed in $\text{Al}_x\text{Ga}_{1-x}\text{As}/\text{GaAs}$ ADQWs (closed squares: Ref. 20; open triangles: Ref. 21), the $\text{InAlAs}/\text{GaAs}/\text{InAs}$ AQDP (closed circles: Ref. 19) together with our data (open circles). Dotted lines are guides for the eye.

low excitation densities by poor PL signal-to-noise ratio and by the asymmetric high energy tail of the LQDs emission.

We have also analyzed τ_T as a function of d_{sp} from the transient PL spectroscopy data. This dependence, shown in Fig. 5 on a semilogarithmic scale, can be fitted using a straight line and follows a simple expression for the tunneling time for barrier penetration assuming a square barrier [semiclassic Wentzel-Kramers-Brillouin (WKB) approximation developed for tunneling processes in coupled QWs]:

$$\tau_T \propto \exp[2d_{sp}\sqrt{(2m^*/\hbar^2)(V - E_{sn})}]. \quad (6)$$

Here m^* is the effective mass in the spacer layer, V is the band discontinuity of the conduction band, and E_{sn} is the lowest confinement energy level in SQD energy. The assumption of a square barrier is most difficult for small d_{sp} , since indium segregation during the capping phase will produce a spacer with an InGaAs alloy composition rather than GaAs . This would decrease the height of the barrier and the effective mass, both of which will decrease τ_T . Although In

segregation is expected during GaAs capping, its amplitude will not be significant for InAs deposition at 500 °C and a GaAs capping rate of 1.0 ML/s. In fact, a sharp interface between InAs QDs and GaAs barriers under these growth conditions is often assumed in order to achieve reasonable agreement between calculations and optical characterizations.⁴

The dependence shown in Fig. 5 supports a model for the observed dependence of τ_T on d_{sp} that is based on carrier tunneling. Naturally one would consider this as nonresonant tunneling since neither the electron nor the hole energy levels in the SQDs and the LQDs are aligned. According to the WKB approximation one can refer to the greater propensity for electrons to tunnel compared with holes due to the large difference in their effective masses. Equation (6) predicts that for a d_{sp} of about 8 nm the tunneling time for the holes is more than three orders of magnitude larger than that of the electrons. In the PL experiments, since carriers with a shorter lifetime govern the decay time, the experimentally observed τ_T should be attributed to electron tunneling. In the same Fig. 5(a), the values of τ_T versus d_{sp} are shown for similar InAs/GaAs AQDPs estimated from the ratio of the integrated cw PL intensities of SQDs and LQDs, assuming equal ratio of the excitation rates for both QD layers, as reported in Refs. 4 and 12. The difference in the obtained values of τ_T between our data and the data in Refs. 4 and 12 might be caused by several reasons: First, the difference in radiative lifetime τ_{R1}^{ef} for the single layer samples, which were used as τ_{R1} of the seed layer (1400 ps in our sample in comparison with 600 ps in Ref. 4 and 500 ps in Ref. 4). Second, the reduced accuracy of the integrated PL intensity from the SQDs for small values of d_{sp} used in Refs. 4 and 12. Third, the contribution of the noncorrelated QDs is not taken into account in Refs. 4, 12, and 19, which would lead to an overestimation of the true tunneling time τ_T . Fourth, comparing our results with Refs. 4 and 12 we can expect some difference due to a difference in growth conditions. While the size of the QDs in Ref. 4 are similar to that reported here, the QDs are grown at lower growth rates in Ref. 12 and are significantly larger.

A comparison with InAlAs/GaAs/InAs AQDPs¹⁹ as well as Al_xGa_{1-x}As/GaAs ADQWs,^{20,21} in which electron tunneling was observed, is displayed in Fig. 5(b). Measured values of τ_T are plotted as a function of the quantity $D = d_{sp} \sqrt{(2m^*/\hbar^2)(V - E_{sn})}$ in order to account for the different structure parameters in InAs, GaAs, and AlInAs. For our structure we used the value of the energy difference $V - E_{sn}$ between the electron ground state in SQD and the GaAs conduction-band edge to be about 110 meV following the data in Ref. 22. An important comment should be made on the mechanisms underlying inter-dot carrier transfer. In contrast to the ADQW structures, the vertically aligned AQDPs three-dimensional shape of the InAs dots makes the definition of d_{sp} somewhat difficult. The uniformity of the dots leads to statistical variations (especially in the case of weakly correlated QD pairs) which requires us to introduce an effective tunnel barrier thickness d_{sp}^{eff} defined as the average distance between the top of QDs in the seed layer and the bottom of the second layer. So in presenting our data in Fig. 5(b) we used d_{sp}^{eff} by taking into account the average dot

height of ~ 4 nm determined from STM images of uncapped single layer 1.8 ML samples.²³

As can be seen in Fig. 5(b), the transient data for the InAlAs/GaAs/InAs AQDP¹⁹ (the only electron tunneling time τ_T directly measured in AQDP to our knowledge) and the ADQW^{20,21} (one of the several transient measurements with similar results) indicate a difference in tunneling time by one order-of-magnitude. (Our data revise the results of Ref. 19 over an even broader range of d_{sp}^{eff} .) The origin for this difference is not well-understood. One explanation¹⁹ is that a longitudinal optical phonon assists the electron tunneling and, therefore, results in a phonon bottleneck for the AQDP. Here we suggest an alternative explanation. For ADQWs the tunneling rate must be calculated over a significant number of final degenerated and nearly degenerated states while for AQDPs the final state is well-defined. This alone could explain the longer tunneling time for the AQDP and is consistent with the fact that in our experiments the tunneling time was insensitive to the energy mismatch between the SQDs and the LQDs.

Let us turn to a discussion of the underlying tunnel mechanisms. The tunneling is logically considered nonresonant tunneling, since electrons (holes) are clearly localized in both the SQDs and LQDs and their corresponding energy levels are not aligned significantly. In principle it could be that both the separate transfer of electrons (holes) and the actual transfer of excitons play a role. Since the energy separations between excited states and ground states of the QDs are large (~ 70 meV), nonresonant tunneling by emission of optical phonons rather than acoustical phonons takes place. Our data gives evidence of electron transfer, while the tunneling time of heavy holes is estimated to be at least one order of magnitude larger than that of electrons due to the larger effective mass. This electron transfer can be interpreted in terms of a transfer from a direct $X_{e_1hh_1}$ into an indirect “cross” exciton state $X_{e_2hh_1}$ (in real space), where an electron is located in the e_2 state of LQDs. Meanwhile, the heavy hole occupies the hh_1 state of SQDs. However, the low recombination effectiveness, as well as the substantially longer transfer time for the hole, efficiently suppresses PL from the indirect exciton state. One would expect rapid relaxation of the $X_{e_1hh_1}$ exciton into the direct $X_{e_2hh_2}$ exciton due to the Coulomb potential that is attracting the hole into LQDs state. This is the case for a comparatively thin barrier. In our case the charged carriers attract carriers of the opposite sign more efficiently in their corresponding layers, thus creating a new pair of direct excitons placed in adjacent layers. These excitons are taken into account by the third term in Eqs. (1). Appearance of an exciton in the LQD of the second layer makes the probability of tunneling of an additional electron from SQD significantly smaller, thus for a moment decoupling the AQDP. This process is taken into account by the second term in Eqs. (1). Together, this simple microscopic model is in a good agreement with the experimental data both for the cw PL data and for the time-resolved PL and does a good job describing the real physical picture in the bilayer system of coupled QDs.

Analyzing the experimental results above, we assumed tacitly that the carriers from the SQDs tunnel immediately

into the ground states of the LQDs thus neglecting the role of the LQDs excited states in the carrier kinetics. However, the energy separation between the ground states of the SQDs and the LQDs exceeds significantly the energy separation between the excited states of LQDs and the ground states of SQDs resulting, in turn, in the predominant carrier tunneling into the excited states of LQDs [Fig. 1(b)]. In what way could available LQDs excited states modify the description of carrier transfer given above? In order to clarify this situation we modified our model to include the possibility for tunneling into the excited state of LQDs. Thus the rate Eqs. (1) now take the form:

$$\begin{aligned} \frac{dn_1(t)}{dt} &= -\frac{n_1(t)}{\tau_{R1}} - \frac{n_1(t)[N_2 - n_2(t)]}{N_2\tau_T} - \frac{n_1(t)[N_2^{exc} - n_2^{exc}(t)]}{N_2^{exc}\tau_T^{exc}} \\ &\quad + G_1[N_1 - n_1(t)]/N_1, \\ \frac{dn_2^{exc}(t)}{dt} &= -\frac{n_2^{exc}(t)}{\tau_{R2}^{exc}} - \frac{n_2^{exc}(t)[N_2 - n_2(t)]}{N_2\tau_2^{int}} \\ &\quad + \frac{n_1(t)[N_2^{exc} - n_2^{exc}(t)]}{N_2^{exc}\tau_T^{exc}} + G_2^{exc}[N_2^{exc} - n_2^{exc}(t)]/N_2^{exc}, \\ \frac{dn_2(t)}{dt} &= -\frac{n_2(t)}{\tau_{R2}} + \frac{n_1(t)[N_2 - n_2(t)]}{N_2\tau_T} + \frac{n_2^{exc}(t)[N_2 - n_2(t)]}{N_2\tau_2^{int}} \\ &\quad + G_2[N_2 - n_2(t)]/N_2, \end{aligned} \quad (7)$$

where $n_2^{exc}(t)$ represents the carrier density at time t in the excited energy levels of the LQDs and N_2^{exc} is the total density of first excited states (generally degenerate) in LQDs that are coupled to SQDs in the AQDPs. The third term of the first equation in Eqs. (7) describes the carrier transfer from the ground states of SQDs to the excited states of LQDs due to tunneling τ_T^{exc} . The factor $[N_2^{exc} - n_2^{exc}(t)]/N_2^{exc}$ defines the fraction of unoccupied excited states of LQDs, which are available for tunneling from the ground states of the SQDs within the AQDP. The middle equation of Eqs. (7) describes the population change in the excited states of the LQDs. Here the radiative lifetime of the excited state is defined as τ_{R2}^{exc} , while τ_2^{int} is the time of interlevel relaxation in the LQDs due to carrier relaxation from the excited states to the ground states of the LQDs. G_2^{exc} is the carrier generation rate in the excited states of the LQDs. The set of Eqs. (7) also takes into account the state filling in the excited and ground states of the LQDs as well as the ground state of the SQDs. For the case of low excitation densities

$$n_2 \ll N_2, \quad n_2^{exc} \ll N_2^{exc}, \quad \text{and } n_1 \ll N_1, \quad (8)$$

corresponding to the experimental conditions, Eqs. (7) reduce to

$$\begin{aligned} \frac{dn_1(t)}{dt} &= -\left(\frac{1}{\tau_{R1}} + \frac{1}{\tau_T} + \frac{1}{\tau_T^{exc}}\right)n_1(t) + G_1, \\ \frac{dn_2^{exc}(t)}{dt} &= -\left(\frac{1}{\tau_{R2}^{exc}} + \frac{1}{\tau_2^{int}}\right)n_2^{exc}(t) + \frac{1}{\tau_T^{exc}}n_1(t) + G_2^{exc}, \end{aligned}$$

$$\frac{dn_2(t)}{dt} = -\frac{n_2(t)}{\tau_{R2}} + \frac{n_1(t)}{\tau_T} + \frac{n_2^{exc}(t)}{\tau_2^{int}} + G_2. \quad (9)$$

Let us assume a reasonable condition $\tau_{R2} \approx \tau_{R2}^{exc}$ and add second and third equations in Eq. (9). In this case the set of Eqs. (9) reduces again to the simple three-level model

$$\begin{aligned} \frac{dn_1(t)}{dt} &= -\left(\frac{1}{\tau_{R1}} + \frac{1}{\tau_T^{eff}}\right)n_1(t) + G_1, \\ \frac{d\tilde{n}_2(t)}{dt} &= -\frac{\tilde{n}_2(t)}{\tau_{R2}} + n_1(t)\left(\frac{1}{\tau_T^{exc}} + \frac{1}{\tau_2^{int}}\right) + \tilde{G}_2, \end{aligned} \quad (10)$$

with effective parameters $\tau_T^{eff} = \tau_T\tau_T^{exc}/(\tau_T + \tau_T^{exc})$ and $\tilde{G}_2 = G_2 + G_2^{exc}$ describing the change of total population of LQDs $\tilde{n}_2(t) = n_2(t) + n_2^{exc}(t)$. In this case tunneling parameter τ_T^{eff} describes the carrier transfer from SQDs to LQDs independently, in what LQDs state does carrier occur finally: ground or excited. Such transfer corresponds to formula (6) where no LQDs final state figures after tunneling, but only the SQDs initial state. However, even if a carrier occurs in the LQDs excited state after tunneling from the SQDs ground state it relaxes to the LQDs ground state due to rapid interlevel relaxation in LQDs, $\tau_2^{int} \ll \tau_{R2}^{exc}$.¹⁷ Thus on the time scale ~ 100 ps the effective parameters are determined in our experiments. Under the restrictions implied by the inequalities (8) the three-level model of Eq. (1) adequately describes the AQDPs as independent of the excited states and state degeneracy in a QD. We resume that our analysis correctly reproduces the interlayer carrier transfer in bilayer asymmetric InAs/GaAs quantum dots.

VI. CONCLUSIONS

In summary, the tunneling processes in InAs/GaAs AQDPs were investigated by means of both steady state and time-resolved PL. The dependence of the tunneling time on the thickness of the separation layer is determined. Controlling the spacer thickness within the limits imposed for noticeable vertical correlation it has been possible to tune the carrier dynamics in the SQDs within wide limits from ~ 2500 ps for 60 ML down to ~ 250 ps for the 30 ML GaAs spacer sample. Analysis of the experimental data is performed in terms of rate equations taking into account the peculiarities of the tunneling transfer in the system of AQDPs. It has been shown that it is important to account for the contribution of noncorrelated QDs both in the second layer and in the seed layer of bilayer InAs/GaAs QDs structure for an accurate estimate of τ_T . The dependence of the tunneling times on the barrier thicknesses is in good agreement with the behavior of the tunneling time for barrier penetration calculated in the WKB approximation developed for tunneling processes in coupled QWs. The deduced dependence $\tau_T(d_{sp})$ has been compared with the analogous functions obtained for similar AQDPs and ADQWs systems provided that different barrier heights and effective masses are properly taken into account. The data support a proposed microscopic model of tunneling including the nonresonant

electron transfer from a direct into a cross exciton state, with subsequent generation of two direct excitons in adjacent QDs layers. This process temporarily blocks the tunneling in the AQDPs leading to a saturation of the tunneling channel and enhancement of the SQDs PL signal.

ACKNOWLEDGMENTS

The authors acknowledge the financial support of the National Science Foundation of US (through Grant Nos. PHY-0099496 and DMR-0080054).

*Electronic address: ymazur@uark.edu

[†]On leave from Institute of Semiconductor Physics, National Academy of Sciences of Ukraine, Prospect Nauki 45, 03028 Kiev, Ukraine.

- ¹D. Bimberg, M. Grundmann, and N. N. Ledentsov, *Quantum Dot Heterostructures* (Wiley, Chichester, 1999); M. Bayer, P. Hawrylyak, K. Hinzer, S. Fafard, M. Korkusinski, R. Wasilevski, O. Stern, and A. Forchel, *Science* **291**, 451 (2001).
- ²G. S. Solomon, *J. Electron. Mater.* **28**, 392 (1999).
- ³Yu. I. Mazur, W. Q. Ma, X. Wang, Z. M. Wang, G. J. Salamo, M. Xiao, T. D. Mishima, and M. B. Johnson, *Appl. Phys. Lett.* **83**, 987 (2003).
- ⁴R. Heitz, I. Mukhametzhano, P. Chen, and A. Madhukar, *Phys. Rev. B* **58**, R10151 (1998).
- ⁵I. Mukhametzhano, R. Heitz, J. Zeng, P. Chen, and A. Madhukar, *Appl. Phys. Lett.* **73**, 1841 (1998).
- ⁶R. Heitz, I. Mukhametzhano, A. Madhukar, A. Hoffmann, and D. Bimberg, *J. Electron. Mater.* **28**, 520 (1999).
- ⁷H. Y. Liu, B. Xu, Y. H. Chen, D. Ding, and Z. G. Wang, *J. Appl. Phys.* **88**, 5433 (2000).
- ⁸M. O. Lipinski, H. Schuler, O. G. Schmidt, K. Eberl, and N. Y. Jin-Phillipp, *Appl. Phys. Lett.* **77**, 1789 (2000).
- ⁹P. B. Joyce, E. C. Le Ru, T. J. Krzyzewski, G. R. Bell, R. Murray, and T. S. Jones, *Phys. Rev. B* **66**, 075316 (2002).
- ¹⁰Yu. I. Mazur, X. Wang, Z. M. Wang, G. J. Salamo, M. Xiao, and H. Kissel, *Appl. Phys. Lett.* **81**, 2469 (2002).
- ¹¹J. He, Y. C. Zhang, B. Xu, and Z. G. Wang, *J. Appl. Phys.* **93**, 8898 (2003).
- ¹²E. C. Le Ru, P. Howe, T. S. Jones, and R. Murray, *Phys. Rev. B* **67**, 165303 (2003).
- ¹³R. Sauer, K. Thonke, and W. T. Tsang, *Phys. Rev. Lett.* **61**, 609 (1988).
- ¹⁴M. G. W. Alexander, W. W. Ruhle, R. Sauer, and W. T. Tsang, *Appl. Phys. Lett.* **55**, 885 (1989).
- ¹⁵A. Tackeuchi, Y. Nakata, S. Muto, Y. Sugiyama, T. Usuki, Y. Nishikawa, N. Yokoyama, and O. Wada, *Jpn. J. Appl. Phys., Part 2* **34**, L1439 (1995).
- ¹⁶Yu. I. Mazur, J. W. Tomm, V. Petrov, G. G. Tarasov, H. Kissel, C. Walther, Z. Ya. Zhuchenko, and W. T. Masselink, *Appl. Phys. Lett.* **78**, 3214 (2001).
- ¹⁷S. Malik, E. C. Le Ru, D. Childs, and R. Murray, *Phys. Rev. B* **63**, 155313 (2001).
- ¹⁸J. W. Tomm, T. Elsaesser, Yu. I. Mazur, H. Kissel, G. G. Tarasov, Z. Ya. Zhuchenko, and W. T. Masselink, *Phys. Rev. B* **67**, 045326 (2003).
- ¹⁹A. Tackeuchi, T. Kuroda, K. Mase, Y. Nakata, and N. Yokoyama, *Phys. Rev. B* **62**, 1568 (2000).
- ²⁰T. H. Wang, X. B. Mei, C. Jiang, Y. Huang, J. M. Zhou, X. G. Huang, C. G. Cai, Z. X. Yu, C. P. Luo, J. Y. Xu, and Z. Y. Xu, *Phys. Rev. B* **46**, 16160 (1992).
- ²¹D. H. Levi, D. R. Wake, M. V. Klein, S. Kumar, and H. Morkoç, *Phys. Rev. B* **45**, 4274 (1992).
- ²²N. Horiguchi, T. Futatsugi, Y. Nakata, N. Yokoyama, T. Mankad, and P. M. Petroff, *Jpn. J. Appl. Phys., Part 1* **38**, 2559 (1999).
- ²³Yu. I. Mazur, Z. M. Wang, G. J. Salamo, M. Xiao, G. G. Tarasov, Z. Ya. Zhuchenko, W. T. Masselink, and H. Kissel, *Appl. Phys. Lett.* **83**, 1866 (2003).